**Engineering and Technology Journal**
**Journal homepage:** https://etj.uotechnology.edu.iq

# Electromechanical Design and Manufacturing of Dynamic Buckling Test Rig Under Various Temperature Conditions

**Shaymaa M. Mshattat [a], Hussain J.M Al-Alkawi [b], Ahmed H. Reja [c]**

[a, c] University of Technology-Iraq, Alsina'a street,10066 Baghdad, Iraq.
[b] Bilad Alrafidain University College, Diyala, Iraq.
*Corresponding author Email: eme.19.43@grad.uotechnology.edu.iq

## HIGHLIGHTS

- A thermal buckling test rig was designed and constructed under variable temperatures.
- The buckling properties of the material used are less with increasing temperature.
- The buckling load is reduced under the influence of interaction the load with temperature.

## ARTICLE INFO

**Handling editor:** Muhsin J. Jweeg

**Keywords:**
Test Rig Design
High Temperature
Buckling Test
AA-6061-T6

## ABSTRACT

A column is a structural member that bears an axial compressive load and is more likely to fail due to buckling compared to material strength. Some of these columns work at a high temperature and this temperature affects the behavior of buckling. Therefore, the designer must take this factor (temperature) into consideration. For the purpose of studying the effect of different temperatures on the phenomenon of buckling under compression dynamic loads to evaluate the state of failure for different types of columns, the thermal buckling test device has been designed and manufactured. Using this rig, practical tests can be conducted on solid and hollow columns of different metals and diameters, and thus the safe critical load for the column can be predicted. This device was successful in evaluating the life of the columns made of aluminum alloy (6061-T6) when the buckling interacts with heat. The current study found that rising the temperature increases the failure under the buckling phenomenon.

## 1. Introduction

Any slender bar or member subjected to a compressive load is called strut or column. Piston rods, connecting rods, and side links in forging machines are struts. The failure of such members may occur by pure compression, by buckling, or by a combination of pure combination of pure compression and buckling, depending upon a slenderness ratio (S.R.)[1]. Materials with high-temperature qualities are important in a wide range of applications, including power plant generation equipment, the automobile sector, and space structures. The temperature of these components is almost certain to rise [2]. The main force in columns is compression. The carrying capacity of members diminishes dramatically in a high-temperature ambience. Therefore, research into column stability at elevated temperatures is required [3]. Buckling behaviors of columns at various temperatures had been offered. Maljaars et al. [4] examined flexural buckling of a square hollow section and an I-shaped section aluminum columns exposed to a high temperature. They developed a finite element model (FEM) and compared it with practical results. They found that (FEM) showed sufficiently accurate results to describe flexural buckling of aluminum columns subjected to an elevated temperature. They also showed that the simple calculation model for flexural buckling of temperature aluminum columns exposed to a temperature in Eurocode9 does not give an accurate prediction of the buckling resistance in temperatures. The authors proposed a new method of an alternative design model, which takes into calculation the shape of the stress–strain relationships of aluminum alloys at high temperatures. Predictions of this model have good agreement with those of (FEM). Kadhim K. Resan et al. [5] studied the buckling behavior of slender fiber reinforced polymer columns subjected to static axial loading under various temperatures. They used two groups of composite materials, group (A) consisting of Perlon fiber as reinforcement with acrylic resin as a bonding matrix, while group (B) consists of a combination of Perlon and Carbon fibers as reinforcement. The test results showed that the value of the critical load and Young's Modulus decreases with increasing the temperature for both groups and the difference in critical buckling load at room temperature of (50 $^{o}$C) was (63.8 % and 62.1%) for groups (A and B), respectively. Seo, Won et al. [6] studied the change in the elastic buckling characteristics of a steel circular tube in fire the using finite element analysis. The parameters of the elastic buckling



http://doi.org/10.30684/etj.v40i1.2276
Received 09 July 2021; Accepted 28 September 2021; Available online 25 January 2022
2412-0758/University of Technology-Iraq, Baghdad, Iraq

behaviors' analysis used were, diameter–thickness ratio, fire exposure area, and fire scenarios. Such parametric studies were performed with a critical load ratio to initial buckling strength corresponding to the exposure time. They showed that the entire surface of the circular steel tube was exposed to high temperatures, and the elastic buckling strength decreased by 20% within 10 minutes from the start of fire. In case 50% of the area is exposed to fire, the strength decreased to 20% or less for all models in 100 minutes. In case 12.5% of the area is exposed to fire, the strength decreased to 30% or less in 100 minutes and they also showed that local buckling can lead to global failure. Jiang, Xiong et al. [7] examined the behavior of buckling of aluminum alloy columns under high temperature conditions. They tested 108 aluminum columns under an axial static load at elevated temperatures and ambient temperatures, including 60 rectangular tubes and 48 circular tubes. They compared between the experimental results and the values calculated from the ANSYS. Depending on the statistical regression method (FE results and Perry-Robertson formulation), they proposed formulae to estimate the stability coefficients of aluminum alloy columns under fire conditions. The proposed formulae were compared with the test results and the stability coefficients from existing codes. It was found that the proposed formulae were accurate to predict the ultimate loads of aluminum alloy columns at elevated temperatures of (20–300◦C). H. Ma, Q.Hou, et al. [8] performed the material and axial compression tests at various temperatures for H-section 6082-T6 aluminum alloy columns. They showed the material properties, load–strain curves, load–displacement curves, and ultimate bearing capacity of each member at different temperatures. They proposed formula to calculate the stability coefficient of the columns under axial compression at different temperatures. The test results were compared with the fitting formula, Chinese Code (GB), and European Code (EC9). The comparison results demonstrated that the fitting formula can provide a more accurate stability coefficient for the columns at different temperatures.

The main objective of this research is to design and manufacture a thermal-buckling test device under rotation case and axial compressive load, through which it is possible to study the influence of the interaction of the load with temperature on the buckling behavior of columns and predict the critical buckling load and the safety factor for the loaded part to make it work with a longer life.

## 2. Experimental work

### 2.1 General layout of the dynamic buckling test rig at elevated temperatures

The test rig is collected from the following components in order to create a modern and a unique system for studying the effect of the composite factor, which is the load and temperature simultaneously on a column. This rig can handle solid and hollow specimens with diameters ranging from 2 to 14mm. As a result, specimens can be examined with various slenderness ratios of (short, intermediate, and long) under different temperatures using this test apparatus. Figure 1 shows the schematic diagram and the actual thermal buckling test machine. The parts of the designed test rig are as follows:

Mechanism of torsion.
Mechanism of pressure.
Electric oven.
Buckling failure measuring device.

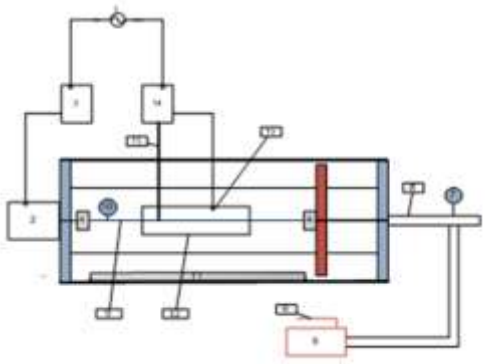

**Figure 1:** A Schematic diagram of the whole thermal buckling test device

**Figure 1:** B Actual thermal buckling test device

The components of the test-rig indicated in the schematic diagram of Figure 1-a are as follows:

1) Power switch (on/off).
2) An electrical motor (1.5hp)
3) Digital AC driver.
4) Set of jaws.
5) Hydraulic pump.
6) Hydraulic pump lever.

7) Pressure gauge.
8) Compression screw shaft.
9) Buckling specimen.
10) Dial gauge.
11) Specimen length measurement ruler.
12) Electric oven.
13) Heater.
14) Digital temperature controller.
15) Sensor.

### 2.1.1 Mechanism of torsion

The torsion system consists of:

a) An electrical motor (1.5hp) connected to one of the jaws that hold the sample, as the motor rotates at different speeds from 50 up to 1500 rpm through the digital AC driver.
b) A set of jaws: is the jaws are made of steel. To fix the sample, the jaw was made with groves according to a unique design.
c) A digital AC driver (model invt: GD20-1R5G-52) in which the speed of the motor is controlled by frequency control and is called variable frequency drive where the current passes through three phases, the first stage is to convert the alternating current into direct current by a group of diodes and the second stage converts the output DC current into a pure DC current through the capacitor. The third and final stage is the conversion of the direct current into an alternating current by a group of transistors and it is at variable frequencies. Hence, the voltage velocity is controlled by frequency control [9]. Figure 2 shows the parts of the torsion system.

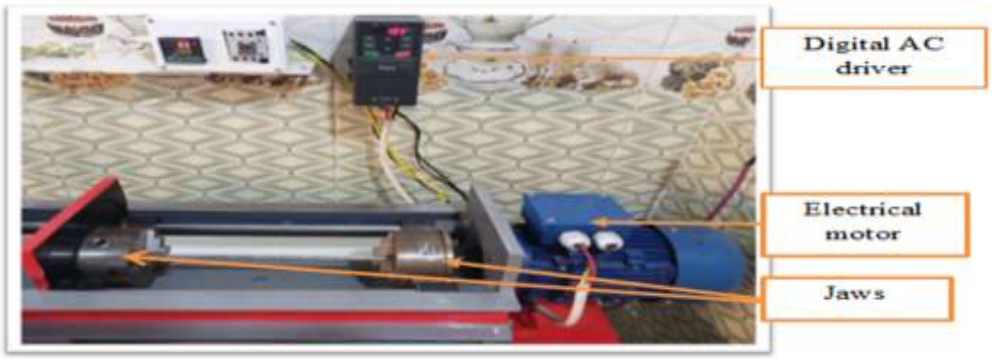


**Figure 2:** The torsion system

### 2.1.2 Mechanism of pressure

The compression load system consists of a hydraulic pump manually operated by a lever. This pump gives the highest pressure of up to 160 bars. It is read on a pressure gage connected to the impeller tube of the pump. The pressure reaches the second jaw that holds the end of the sample through a hollow axis connecting the pump and the sample. Figure 3 illustrates the compression system.

### 2.1.3 Electric oven

To examine the temperature effect on the buckling columns, the electric oven is designed and manufactured. It is a thermal device that generates heat to heat the spaceman within the chamber, causing the sample to alter mechanically. The oven was built and configured as a laboratory furnace, with a maximum temperature of 400°C. The materials utilized to make the box were sourced locally. The electric oven consists of the following parts:


**Figure 3:** Parts of the compression system

#### 2.1.3.1 Chamber

It consists of two layers of galvanized iron with dimensions of (300mm * 250mm * 180mm), between them there is a layer of thermal insulation.

#### 2.1.3.2 Heater of (900 watts)

It is used to produce the heat and raise the temperature to the required temperature.

#### 2.1.3.3 Sensor type (K)

The metals Ni-Cr (Chromel) and Ni-Al (Alumel) are used to make a K type thermocouple, as shown in Figure (4). It's a low-cost device that's also one of the most often used thermocouples. The temperature range is (-180°C to +1350°C). The sensitivity is around 42 μV/℃ [10]. A sensor in a stainless-steel sheath with a (1/6) inch diameter is put into the oven to measure the temperature of the sample and then it sends this information to the controller.

#### 2.1.3.4 Digital temperature controller

A controller model (TOKY: A1208) shown in Figure 4 controls the heat flow to the load by adjusting the power output from the heat source according to the information received from the sensor. The controller compares the temperature measured by the sensor to the required load temperature (the set point), and the device's output is either on or off, with no in-between state. An on-off controller will switch the output only when the temperature crosses the set point. For heating control, the output is on when the temperature is below the set point, and the output is off when the temperature is above the set point. Since the temperature crosses the set point to change the output state, the process temperature will be cycling continually, going below and above the set point [11].

#### 2.1.3.5 Contractor

A contactor is a set of high-current contacts controlled by a solenoid to provide an on/off function. A low voltage, low current signal is often required by the solenoid. As a result, with a very light cable and a high degree of safety, it may be operated from a far location. Commercial contactors, like the ones illustrated in Figure 4, come in a variety of designs, voltages, and currents. Commercial contactors with current ratings of up to 200 amps per pole are popular [12].


**Figure 4:** Parts of the electric oven

### 2.1.4 Buckling failure measuring device

The device used to measure buckling and failure is:

#### 2.1.4.1 Digital dial gauge

Digital dial gauges are crucial tools for properly measuring very small and diminutive liner distances. Models of analog and digital dial gauges are available, depending on the application. The benefits of using a digital dial gauge are as follows:

a) Good sensitivity of up to 0.025μ m (1μ in), accuracy, and good responsiveness.
b) Sensitivity.
c) The ease with which it can be used.
d) Reducing human mistake.
e) Data that can be presented in a variety of forms is read.

The digital dial gauge activates when the spindle touches the specimen and changes its displacement. This shift in displacement is reflected in digital readings.

#### 2.1.4.2 Magnetic base

The dial gauge is mounted to a magnetic base (Mitutoyo) type to be able to install it in different areas and allowing adjusting it to different directions and positions. Figure 5 shows the whole system.


**Figure 5:** Buckling failure measuring device

## 2.2 Buckling samples

In this research, 18 samples are selected of long solid columns made of aluminum alloy (6061-T6) with different lengths and diameters as presented in Figure 6. Table 1 shows the dimensions of the sample that was used.

**Table 1:** Initial parameters and dimensions of the columns

| No. | D mm | L mm | Le mm | A mm2 | I mm4 | r min mm |
|---|---|---|---|---|---|---|
| 1 | 8 | 450 | 315 | 50.265 | 201.06 | 2 |
| 2 | 8 | 400 | 280 | 50.265 | 201.06 | 2 |
| 3 | 8 | 350 | 245 | 50.265 | 201.06 | 2 |
| 4 | 10 | 450 | 315 | 78.539 | 490.87 | 2.5 |
| 5 | 10 | 400 | 280 | 78.539 | 490.87 | 2.5 |
| 6 | 10 | 350 | 245 | 78.539 | 490.87 | 2.5 |

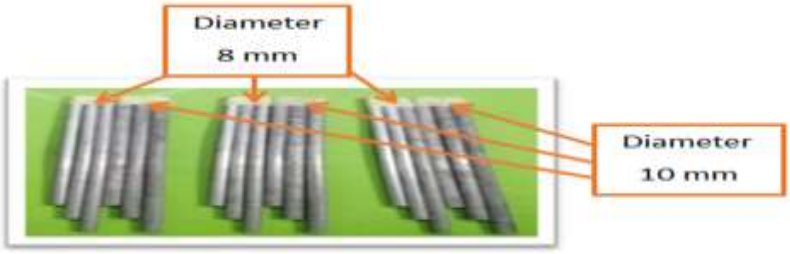


**Figure 6:** Buckling samples

## 2.3 Composition of chemicals

Table 2 shows the chemical composition that was carried out in State Company for Inspection and Engineering Rehabilitation (SIER).

**Table 2:** Chemical composition analysis obtained for AA 6061-T6

| 6061-T6 Al-alloy | Al% | Cr% | Cu% | Fe% | Mn % | Si% | Ti% | Zn% |
|---|---|---|---|---|---|---|---|---|
| ASTM B-211 | Balance | 0.04-0.35 | 0.15-0.4 | 0.4-0.8 | Max. 0.15 | 0.4-0.8 | Max. 0.15 | Max. 0.25 |
| Experimental | Balance | 0. 17 | 0.282 | 0.46 | 0.12 | 0.57 | 0.1 | 0.18 |

## 3. Thermal-buckling test results

Firstly, six samples are selected of solid columns made of AA (6061-T6) presented in Figure 6 with different lengths and diameters. The experimental critical buckling load (Pcr) under increasing compressive dynamic loading at room temperature can be shown in Table 3.

**Table 3:** Results of columns under increasing buckling load at room temperature

| No. | D mm | L mm | $L_e$ mm | S.R. | δcr mm | $P_{cr}$ Exper.(N)at R.T. |
|---|---|---|---|---|---|---|
| 1 | 8 | 450 | 315 | 157.5 | 6.5 | 663.4 |
| 2 | 8 | 400 | 280 | 140 | 6.1 | 733.8 |
| 3 | 8 | 350 | 245 | 122.5 | 5.3 | 904.7 |
| 4 | 10 | 450 | 315 | 126 | 6.4 | 1483.7 |
| 5 | 10 | 400 | 280 | 112 | 6.1 | 1679.9 |
| 6 | 10 | 350 | 245 | 98 | 4.6 | 2150.9 |

A buckling test at elevated temperatures was conducted by taking 12 columns of AA (6061-T6) specimens. They have been tested under different compressive dynamic loading values with different levels of elevated temperatures (100°C and 200°C). Table 4 illustrates the test critical buckling load at various temperatures.

**Table 4:** Results of columns under increasing buckling load at elevated temperatures

| No. | D mm | L mm | $L_e$ mm | δcr mm at(100and200C) | $P_{cr}$ Exper.(N)at100°C | $P_{cr}$ exper.(N)at200°C |
|---|---|---|---|---|---|---|
| 1 | 8 | 450 | 315 | 6 | 472.4 | 301.6 |
| 2 | 8 | 400 | 280 | 6 | 550.7 | 371.8 |
| 3 | 8 | 350 | 245 | 6 | 712.9 | 475.6 |
| 4 | 10 | 450 | 315 | 6 | 1326.7 | 811.3 |
| 5 | 10 | 400 | 280 | 6 | 1452.3 | 984.6 |
| 6 | 10 | 350 | 245 | 4 | 1781.9 | 1267.3 |

## 4. Discussion

From Tables 3 and 4, it was noted that the slenderness ratio (S.R.) of a column has a significant influence on the critical buckling load. When the (S.R.) decreases, the critical buckling load increases. As a result, failure stress increases as the slenderness ratio approaches intermediate columns. This finding agreed with what was found by references [13 and 14]. When the value of the diameter increases, the failure stress increases. Increasing the diameter with a constant length causes the column to behave as an intermediate column and not as a long one, and vice versa, whenever the diameter decreases with a constant length, the direction goes to the long columns. Therefore, specimens that have diameters of (D=10 mm) require more load to attain failure than specimens that have diameters of (D=8 mm), as illustrated in Figure 7.

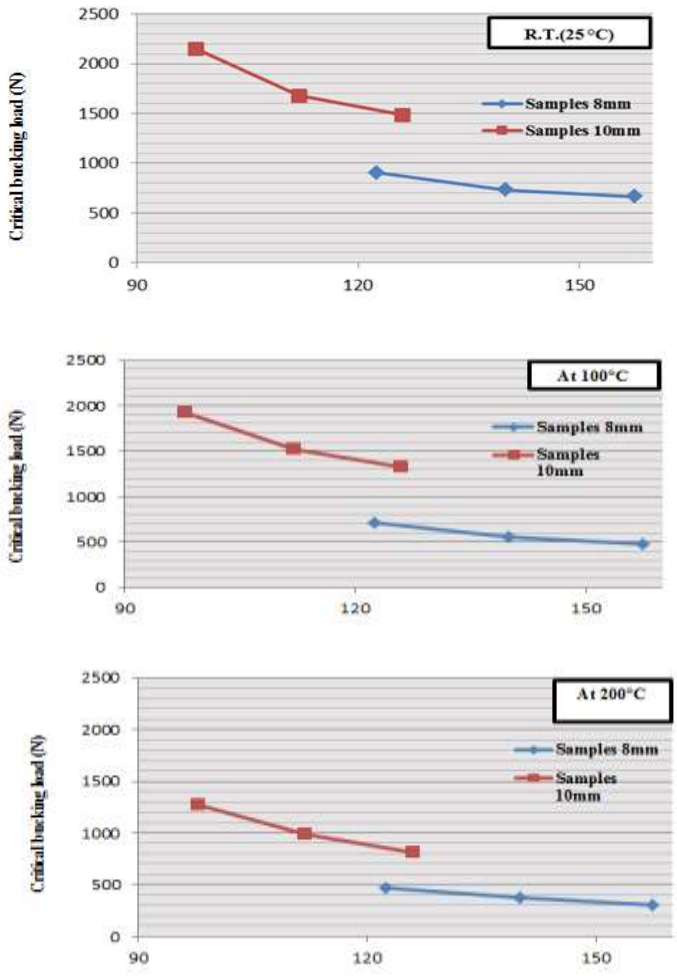


**Figure 7:** Variation of critical buckling load with slenderness ratio at various temperatures

When the compressive stress is progressively raised, it reaches the point where the column is beginning to buckle. The critical buckling load is defined as the load that causes the column to buckle. In this case, the column can be described as an elastic instability.

From Tables 3 and 4, it is clear that a high temperature in general has the overall effect on the structure and it eliminates the strength of material. In other words, a high temperature weakens the structure and decreases its mechanical properties, and this result is in line with the references' conclusions in [15 and 16], and this leads to decrease the critical buckling load ($P_{cr}$) of the aluminum alloy specimens. The buckling behavior of AA 6061-T6 under various temperatures can be seen in Figure 8.

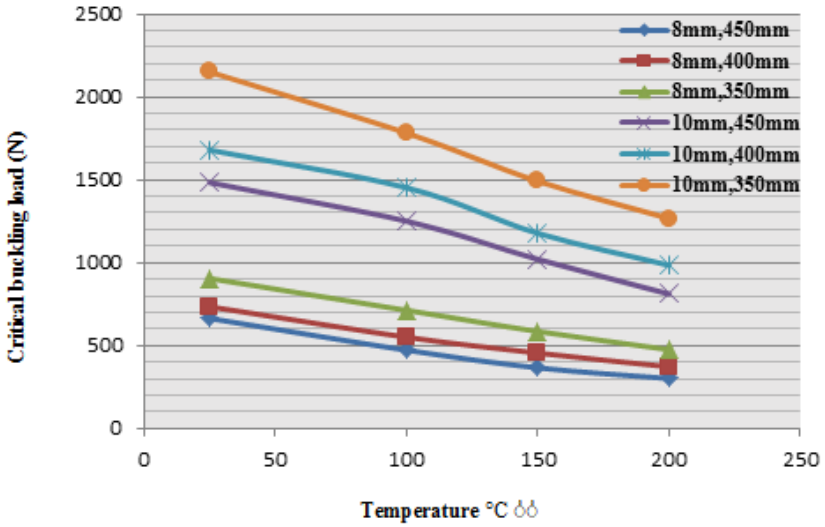


**Figure 8:** Variations of the critical buckling load with temperature

The reduction percentages in the above buckling properties can be illustrated in Table V. The influence of the interaction of the load with temperature can be obviously noted on the buckling behavior of columns as presented in Table. The values of these critical buckling loads are reduced from (9.86% to 28.79% and 41.08% to 54.54%) for columns tested at elevated constant temperatures of (100°C and 200°C), respectively.

**Table 5:** Reduction percentage in the critical buckling load under high temperatures

| No. | D mm | L mm | Reduction in($P_{cr}$) at 100°C | Reduction in($P_{cr}$) at 200°C |
|---|---|---|---|---|
| 1 | 8 | 450 | 28.79% | 54.54% |
| 2 | 8 | 400 | 24.95% | 49.33% |
| 3 | 8 | 350 | 21.20% | 47.43% |
| 4 | 10 | 450 | 10.58% | 45.32% |
| 5 | 10 | 400 | 9.86% | 41.39% |
| 6 | 10 | 350 | 10.46% | 41.08% |

## 5. Conclusions

The conclusions are divided to many points as follows:

1) A new high temperature buckling test rig was successfully designed and constructed under variable temperatures.
2) This device will assist students and researchers in universities to examine the buckling behavior of columns with various slenderness ratios under increasing load and different temperatures with accurate results.
3) For a given length and diameter of AA6061-T6 column, increasing the temperature leads to reduce the reduction in the critical load (Pcr), because the high temperature in general has the overall effect on the structure and it eliminates the strength of material.
4) The reduction percentages of the value of critical buckling loads were (28.79% and 54.54%) for columns tested at elevated constant temperatures of (100 and 200°C), respectively in comparison with the room temperature.

### Author contribution

All authors contributed equally to this work.

### Funding

This research received no specific grant from any funding agency in the public, commercial, or not-for-profit sectors.

### Data availability statement

The data that support the findings of this study are available on request from the corresponding author.

### Conflicts of interest

The authors declare that there is no conflict of interest.

## References

**[1]** R. L. Mott and E. M. Vavrek, Machine Elements in Mechanical, Sixth Edit. Pearson, (2018).

**[2]** R. Fortune, Elevated Temperature Effects on the Mechanical Properties of Age Hardened 6xxx Series Aluminum Alloy Extrusions, The Faculty of The Materials Engineering Department, California State University, (2015).

**[3]** M. F. Akhtar, Numerical investigation of high strength structural steel gravity columns at elevated temperature A, The University of Cincinnati, (2020).

**[4]** J. Maljaars, L. Twilt, and F. Soetens, Flexural buckling of fire exposed aluminium columns, Fire Saf. J., 44 (2009) 711–717. https://doi.org/10.1016/j.firesaf.2009.02.002

**[5]** K. K. Resan and M. H. Ali, Effect of Temperature on Buckling of Composite Materials Column Theoretical Analyses , Al-Nahrain Journal for Eng. Sciences (NJES) 20 (2017) 511–519.

**[6]** J. Seo, D. Won, W. Park, and S. Kim, Buckling Behavior of Circular Steel Tubes under Fire, Key Eng. Materials, 763 (2018) 270–278, doi: 10.4028/www.scientific.net/KEM.763.270.

**[7]** S. Jiang, Z. Xiong, X. Guo, and Z. He, Buckling behaviour of aluminium alloy columns under fi re conditions, Thin Walled Struct., 124 (2018) 523–537,. doi: 10.1016/j.tws.2017.12.035.

**[8]** H. Ma, Q. Hou, Z. Yu, and P. Ni, Thin-Walled Structures Stability of 6082-T6 aluminum alloy columns under axial forces at high temperatures, Thin-Walled Struct., 157 (2020) 107083,. doi: 10.1016/j.tws.2020.107083.

**[9]** D. M. Bezesky and S. Kreitzer, NEMA Application Guide for AC Adjustable Speed Drive Systems, NEMA standards, The association of electrical equipment and medical imaging manufacturers,(2007) (2001) 1–10.

**[10]** Douglas Self, Audio Engineering. Elsevier, (2009).

**[11]** M. Fardadi, A. S. Ghafari, and S. K. Hannani, PID Neural Network Control of SUT Building Energy Management System, Proceedings 2005 IEEE/ASME International Conference on Advanced Intelligent, Mechatronics, pp. 24–28, (2005).

**[12]** B. S. ELLIOTT, Electromechanical devices & components illustrated sourcebook. McGraw-Hill, (2007).

**[13]** H. A. Aziz, An Appraisal Of Euler And Johnson Buckling Theories Under Dynamic Compression Buckling Loading ., The Iraqi Journal for Mechanical and Material Eng., 9 (2009) 173–181.

**[14]** M. Avcar, Elastic buckling of steel columns under axial compression, American Journal of Civil Eng., 2 (2014) 102–108, .doi: 10.11648/j.ajce.20140203.17.

**[15]** M. Su and B. Young, Thin-Walled Structures Material properties of normal and high strength aluminium alloys at elevated temperatures, Thin Walled Struct., 137 (2019) 463–471, .doi: 10.1016/j.tws.2019.01.012.

**[16]** P. T. Summers et al., Overview of aluminum alloy mechanical properties during and after fires, Fire Sci. Rev., no. December 2015, (2016). doi: 10.1186/s40038-015-0007-5.